Analyzing the Effective Throughput in Multi-Hop IEEE 802.11n Networks

Simon Frohn, Sascha Gübner, and Christoph Lindemann
Department of Computer Science
University of Leipzig
Johannisgasse 26, 04103 Leipzig, Germany

{frohn, guebner, cl}@rvs.informatik.uni-leipzig.de

Abstract—**In this paper we characterize the effective throughput for multi-hop paths in IEEE 802.11n based wireless mesh networks. We derive an analytical model capturing the effects of frame aggregation and block acknowledgements, features found in the new IEEE 802.11n standard. We describe the throughput at MAC layer as a function of physical data rate, error rate, aggregation level and path length. While being mathematically tractable, the proposed model is flexible enough to account for complex and realistic error characteristics of the wireless channel, such as long-term fluctuations and burstiness. We further show how to integrate the well-known Gilbert-Elliot channel model into our model and evaluate both models in our indoor wireless testbed.**

Keywords: IEEE 802.11 wireless networks; Analytical model; Measurement study

I. Introduction

In recent years, wireless mesh networks became increasingly interesting in academia and industry because they can easily be built with low infrastructure costs despite a huge coverage. Therefore, they are particularly attractive for providing fast and cost-efficient coverage for hard-to-wire areas. Further areas of application include disaster scenarios, wireless machine-to-machine communication, and wireless video surveillance. The IEEE 802.11n standard [1] is the first IEEE 802.11 amendment to introduce a physical layer based on Multiple-Input and Multiple-Output (MIMO) transmission scheme, providing data rates up to 600Mbit/s and increased tolerance to interference. These features make IEEE 802.11n a promising technology for building carrier grade wireless mesh networks. The high data rates provided by the IEEE 802.11n physical layer can only be harnessed at upper layers if medium access is efficient. Therefore, IEEE 802.11n introduces frame aggregation. Using frame aggregation, multiple subframes can be transmitted in sequence with the overhead for medium access arising only once. One option allows each subframe transmitted in an aggregated frame to be guarded by an own Cyclic Redundancy Check (CRC) checksum, i.e. the IEEE 802.11n Medium Access Control (MAC) at the receiver can extract individual subframes even if parts of the aggregated frame are erroneous due to lossy channel conditions. Upon reception of an aggregated frame, the receiver can send a BlockAck control frame to acknowledge all correctly received subframes.

For the design of data transport protocols, an understanding of the effective throughput of IEEE 802.11n is required. An appropriate analytical model has to consider the aggregation capabilities as well as partial retransmits occurring in IEEE 802.11n. Furthermore, the characteristics of the wireless channel as a scarce resource shared among all mesh nodes within their radio transmission range has to be considered.

In this paper we characterize the effective throughput for multi-hop paths in IEEE 802.11n based wireless mesh networks. We derive an analytical model based on a Markov chain capturing the effects of frame aggregation and block acknowledgements, features found in the new IEEE 802.11n standard. Our model calculates the expected number of retransmissions by estimating the amount of subframes to be retransmitted under a given channel model. With our Markov model, we are able to describe the throughput at MAC layer as a function of physical data rate, error rate, aggregation level and path length. Furthermore, we show how to integrate the well-known Gilbert-Elliot channel model into our model to take complex error characteristics into account. We develop a Markov chain counting the correctly received number of subframes in an aggregated frame of arbitrary size under the Gilbert-Elliot channel model. This way, while being mathematically tractable, the proposed model is flexible enough to account for realistic error characteristics of the wireless channel, such as long-term fluctuations and burstiness. Subsequently, we validate our model through simulations for multi-hop communication on a chain topology in IEEE 802.11n. We hereby show that our analytical model is able to closely estimate the effective throughput on these topologies.

Furthermore, we introduce our Indoor MIMO testbed and quantitatively show therein, that the Gilbert-Elliot channel model is able to describe error behavior in IEEE 802.11n communication. We employ the Baum-Welch algorithm to estimate the parameters of the underlying Gilbert-Elliot channel model and show that it is able to model error characteristics like mean subframe error rate, distribution of error burst length, and the distribution of the burst length of correctly received subframes in our testbed. Finally, we evaluate our proposed Markov model by estimating the throughput of different testbed links.

The remainder of this paper is organized as follows. Section II summarizes related work on analytical models for IEEE 802.11n and data transport optimization for wireless mesh networks, Section III gives a short overview regarding the frame aggregation and block acknowledgement features of IEEE 802.11n. In Section IV, we introduce our analytical model. In Section V we validate our model through simulations and evaluated it further in a real-world indoor testbed in Section VI. Finally, concluding remarks are given.

II. RELATED WORK

Banchs et al. [2] presented an analytical model for the IEEE 802.11e Enhanced Distributed Channel Access (EDCA) medium access scheme. Their model describes the throughput for saturated traffic as a function of interframe spacing and contention window parameters. Based on this model, an optimal EDCA configuration is derived. Bianchi et al. [3] presented a model for the throughput of IEEE 802.11 single-hop links under the assumption of ideal channel conditions and a finite number of terminals. They assumed saturated traffic, i.e. each node always has a frame available for transmission. Engelstad et al. [4] presented an analytical model capturing throughput, delay and frame drop probabilities for both saturated and non-saturated channel traffic. Daneshgaran et al. [5] characterized the throughput of the IEEE 802.11 DCF at MAC layer for non-saturated traffic. Opposed to [2], [3], [4] and [5] we characterize the throughput at MAC layer in the presence of the frame aggregation and block acknowledgements.

Li et al. [6] proposed Aggregation with Fragment Retransmission (AFR). Using AFR multiple subframes are aggregated and transmitted in a single large frame. They presented an analytical model to evaluate the throughput and delay performance of the AFR scheme over noisy channels. They further prove that the zero waiting approach of the AFR scheme can achieve maximum throughput. Based on the analytical model they derived the effective throughput and optimal frame and fragment sizes for single-hop links. Opposed to [6] we also consider multi-hop paths. Furthermore, we do not rely on a specific channel model, rather we provide a flexible analytical framework supporting different channel models.

Chen et al. [7] characterized the bandwidth delay product for wireless multi-hop paths. They obtained a qualitative upper bound for the throughput considering the spatial reuse constraint of the medium. Fu et al. [8] analyzed the effect of pacing for multi-hop wireless networks and proposed a pacing scheme at MAC layer. They showed, that for specific network topologies and traffic patterns, there exists an optimal contention window size for the Transmission Control Protocol (TCP). For the optimal TCP contention window size TCP achieves the highest throughput because of maximum spatial reuse of the shared wireless channel. Opposed to [7] and [8], we obtain quantitative results considering the frame aggregation and BlockAck feature of IEEE 802.11n MAC layer in presence of lossy channel conditions.

Shrivastava et al. [9] analyzed the performance of IEEE 802.11n over single-hop links in a testbed. Karlsson et al. [10] reported on the performance of TCP under different traffic scenarios in the presence of packet aggregation. They found that packet aggregation can significantly increase the performance of TCP in wireless networks. Opposed to [10] and [9], we provide an analytical model considering the frame aggregation capabilities of IEEE 802.11n.

In [11], we presented ScaleMesh a miniaturized dual-radio wireless mesh testbed based on IEEE 802.11b/g and conducted a comprehensive measurement study. We analyzed the effect of channel selection, signal attenuation level, different topologies, and traffic load on network performance. Opposed to [11], we consider frame aggregation in the new IEEE 802.11n standard.

To show the versatility of our framework we employed the widely used channel error model proposed by Gilbert and extended by Elliot [12]. They modeled the wireless channel as a two-state Markov chain that contains a good state, where bit errors occur with a small probability and a bad state with a high bit error rate. As an extension of this model we derived a Markov chain to calculate the probability of how many subframes of an aggregated frame are lost. While being mathematically tractable, the Gilbert-Elliot model takes the often encountered burstiness of the wireless channel into account.

This journal paper extends the conference version [13] with a comprehensive real-world wireless testbed validation and a flexible channel error modeling framework. Furthermore, the underlying assumptions regarding the frame aggregation and block ACK transmissions are discussed in more detail.

III. Background

To keep the paper self contained, we recall the frame aggregation and block acknowledgement features newly introduced by the IEEE 802.11n standard.

With increasing data rates at the physical layer, the time needed for collision avoidance of IEEE 802.11 MAC exceeds the time needed for the transmission of the actual data frame. For example, the single interframe spacing interval (SIFS) is around 16µs, independent of the actual data rate. Same holds for the double interframe spacing interval and the transmit time for the physical header. This is due to compatibility constraints and to provide interoperability between IEEE 802.11 devices operating at different data rates. Due to this constant overhead, the efficiency of the IEEE 802.11 MAC decreases for higher physical data rates. For example, the MAC efficiency is 42% at a physical data rate of 54Mbps, but only 10% for a physical data of 450Mbps [6].

To overcome this deficiency, the IEEE 802.11n standard introduces frame aggregation. Using frame aggregation, multiple frames can be transmitted in a sequence, with the overhead for medium access arising only once. The IEEE 802.11n standard defines two different aggregation schemes: aggregated MAC service data unit (A-MSDU) and aggregated MAC protocol data unit (A-MPDU). The A-MSDU scheme allows to encapsulate multiple packets in a single MAC frame with a single MAC header and a single frame check sequence (FCS). The receiving node can only check the integrity of the whole A-MSDU frame, therefore the whole A-MSDU has to be retransmitted in case of transmission errors. Therefore the A-MSDU scheme is only efficient for the transmissions of multiple small packets, for example TCP acknowledgements packets. Furthermore, the maximum size of an A-MSDU frame is limited to 7935 bytes. Due to these limitations, the A-MSDU scheme appears not to be a promising candidate for the aggregation of multiple TCP data packets. The A-MPDU scheme allows transmitting multiple MAC frames in an aggregated form. In contrast to the A-MSDU aggregation scheme, A-MPDU aggregation takes place after the packet has been encapsulated in a MAC frame. Therefore, each subframe carries its own MAC header and FCS checksum in this scheme. Opposed to the A-MSDU scheme, the receiving node can check the integrity of each subframe individually and only erroneous subframes have to be retransmitted. The maximum size of an A-MPDU frame is limited to 65535 bytes and a maximum of 64 subframes. Between each subframe a MPDU delimiter is inserted to allow the MPDU extraction at the receiving node even when parts of the A-MPDU are erroneous. In the MPDU delimiter the MPDU length, a CRC checksum and the actual delimiter pattern is stored. The CRC checksum is used to protect the MPDU length field against transmission errors. Padding bits may be inserted after each subframe to make each subframe a multiple of 4 bytes in length. The basic structure of an A-MPDU is shown in Figure 1. With the large number of subframes (42 subframes, given a MPDU size of 1534 bytes) and the ability to selectively retransmit erroneous subframes, the A-MPDU scheme appears to be a promising candidate for the aggregation of the multiple TCP data packets.

IEEE 802.11n extends the block acknowledgement extension already known from IEEE 802.11e by introducing a compressed block acknowledgement and an immediate block acknowledgement response option. The compressed block acknowledgement scheme uses an 8 byte bitmap vector to indicate which subframes have been received successfully. Due to the 8 byte limitation the maximum number of subframes for an A-MPDU is 64. In the immediate block acknowledgement scheme depicted in Figure 2 the receiver may send a block acknowledgement in direct response to an A-MPDU (i.e. without contending for a transmission opportunity). The IEEE 802.11n standard enforces the in order delivery of subframes to upper layers. Therefore a correctly received subframe has to be buffered at the receiver until all preceding subframes have been received correctly.

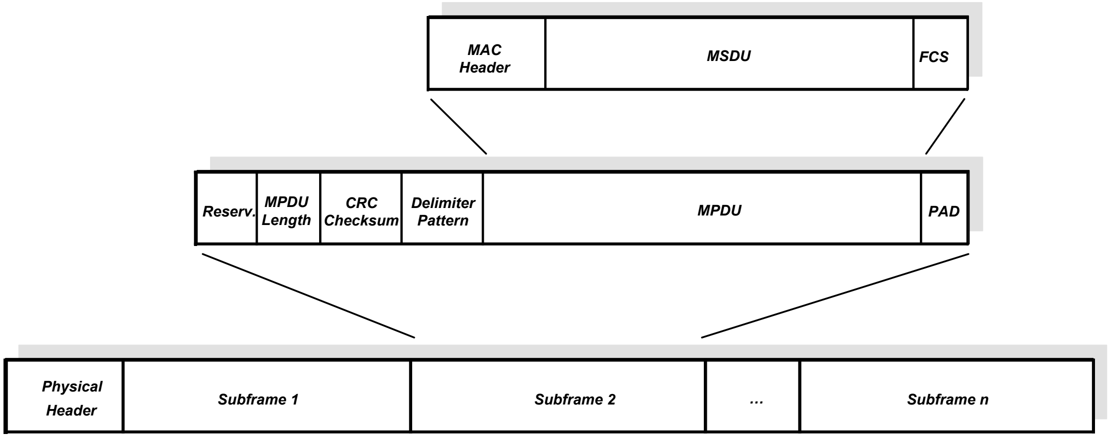

Figure 1. Structure of an IEEE 802.11n A-MPDU.

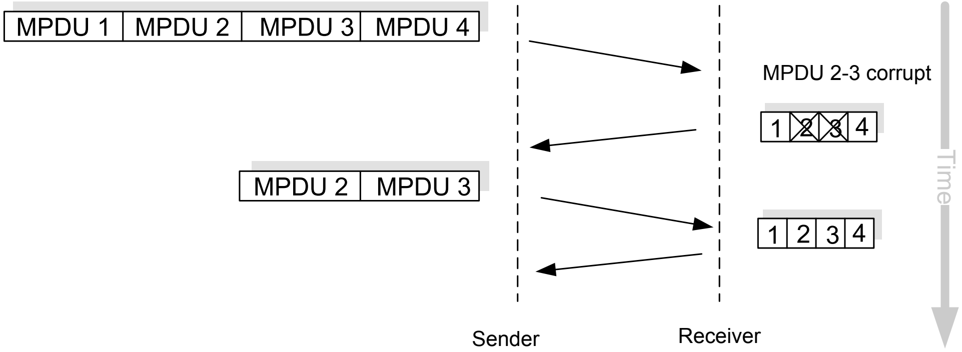

Figure 2. IEEE 802.11n Immediate Block ACK scheme

IV. ANALYTICAL MODEL

A. Model Assumptions

To characterize the effective throughput for multi-hop chains, we consider an arbitrary unicast routing protocol and a single traffic flow from one source to one sink. We consider a physical layer bandwidth of B_{DATA} and a single-channel, single-radio configuration. Consistent with the IEEE 802.11n standard [1] (A-MPDU and HT Immediate BlockAck Extension, Subclause 9.10.7), we assume that up to N subframes can be transmitted in an aggregated frame, with the overhead (i.e. backoff interval, physical header) for medium access arising only once. Upon reception of an aggregated frame, the receiver sends a BlockAck response, where each correctly received subframe is acknowledged. Upon reception of a BlockAck, the sender retransmits all subframes which have not been acknowledged. This procedure is repeated until r_{max} transmission attempts have been made or until all subframes have been acknowledged. Because of the Cylic Redundancy Check performed by the IEEE 802.11 MAC layer, we assume that a frame is discarded if it contains at least one bit error, neglecting the rather unlikely case, where a set of bit failures is not correctly detected because the CRC checksum of the original and defective frame is identical.

To capture the characteristics of the wireless channel as a shared resource, we assume that two nodes can transmit simultaneously, (i.e. without collisions at the receiving nodes due to the hidden terminal problem) if their distance in terms of hops is at least d_{coll}. Therefore, the traffic at intermediate nodes is not saturated and the sender has no new subframes available when subframes have to be retransmitted. A detailed overview of the used model parameters is given in Table I.

TABLE I. MODEL PARAMETERS

Symbol	***Description***
B_{DATA}	Physical layer bandwidth
S	Size of a subframe (in bits)
N	Number of subframes per aggregated frame
r_{max}	Max. number of transmission attempts
S_N	Random variable denoting the number of lost frames
$P_{att}(l)$	Probability that an aggregated frame is fully transmitted in exact l attempts (acc. to (4))
b_{err}	Bit error rate
p_f	Subframe error rate
q	Transition rate from good to bad state
r	Transition rate from bad to good state
b_g, b_b	Bit error rate in good and bad state, resp.
p_g, p_b	Subframe error rate in good and bad state, resp.
$C(l)$	Time required to transmit an aggregated frame in exactly l attempts (acc. to (13))
T_{slot}	Slot time
cw_{min} ,cw_{max}	Min. and max. size of contention window
T_{PHY}	Time to transmit physical header

B. Generic Framework Description

To account for different error characteristics of the wireless channel, we propose a generic framework for calculating the probability that an aggregated frame, consisting of N subframes is fully transmitted after r retransmission attempts. Given the fixed maximum number of retransmission attempts r_{max}, we are further able to calculate the expected number of retransmission needed. Hence, we can derive the expected time needed to fully transfer an aggregated frame over one hop. Therefore, we can calculate the expected throughput. An advantage of our framework is that it can be flexibly combined with different types of wireless channel error models. In subsection C and D we show how to apply the generic framework for two different channel error models, namely the binary symmetric (BS) channel, where bit errors are independently and identically distributed and a channel following the Gilbert-Elliott (GE) model, accounting for the bursty nature of the wireless channel.

The proposed framework models the number of remaining subframes after each transmission attempt by the acyclic discrete time Markov chain (DTMC) depicted in Figure 3. A state (i_1,i_2) of this DTMC defines that i_1 transmission attempts have been made and i_2 subframes are left to be transmitted. The DTMC resides at time 0 in its initial state $(0,N)$ with probability 1, since no transmission attempts have been made and N subframes are left to be transmitted. Then each step in the DTMC accounts for a retransmission attempt until an absorbing state is reached. These states are $(1,0),\ldots,(r_{max},0)$, because all subframes have been submitted and $(r_{max},1),\ldots,(r_{max},N)$, because the number of maximum retransmission attempts have been reached. Given state (i_1,i_2) there are i_2+1 possible transitions, due to the fact, that all i_2 subframes could be transmitted successfully or $1,\ldots,i_2$ subframes could be lost. A transition from state (i_1,i_2) to state (j_1,j_2) can therefore occur if $j_1=i_1+1$ and $j_2\leq i_2$. The transition probabilities can be expressed in the probability matrix

$$\mathbf{P} = [p_{ij}] = P\{X_{n+1} = j \mid X_n = i\} \tag{1}$$

where $i=(i_1,i_2)$ and $j=(j_1,j_2)$. Furthermore, let the random variable S_N denotes the number of lost subframes in an aggregated frame of N subframes. Then the state transition probabilities p_{ij} are given by

$$p_{ij} = \begin{cases} P[S_{i_2} = j_2] & \text{if } j_1 = i_1 + 1 \text{ and } 0 \leq j_2 \leq i_2 \\ 1 & \text{if } i_1 = j_1 = r_{max} \text{ and } i_2 = j_2 \\ 1 & i_2 = j_2 = 0 \text{ and } i_1 = j_1 \\ 0 & \text{else} \end{cases} \tag{2}$$

where $P[S_N=k]$ is the probability, that k out of N subframes are lost and depends on the selected channel error model, described in the next paragraphs. Note further that the probability is 1 for the absorbing states, where either r_{max} retransmission attempts have been reached (first case) or all subframes have been successfully transmitted (second case).

To fully specify the DTMC, the initial distribution π_0 is needed, where no transmission attempts have been done and N subframes are to be transmitted.

Then π_0 is given by

$$\pi_{0,i} = \begin{cases} 1, \text{if } \mathrm{i} = (0,N) \\ 0, \text{else} \end{cases} \tag{3}$$

With this initial distribution and probability matrix $\boldsymbol{P}$ we can calculate the probability, that after l steps k subframes still have to be retransmitted. Using the matrix power function $(\cdot)^l$, we define the time-dependent distribution π_l after l steps by $\pi_l=\pi_0\boldsymbol{P}^l$ where the (l,k)-th element of this vector gives the desired probability.

With these vectors we calculate the probability $P_{att}(l)$ that exactly l transmission attempts are needed to successfully transmit all subframes to the receiver. This probability is later used to derive the expected number of retransmissions and hence the expected amount of time needed to correctly transmit all subframes of an aggregated frame to the receiver. We define $P_{att}(l)$ by

$$P_{att}(l) = \begin{cases} \pi_{l,i} & , i = (l,0) \text{ for } 0 < l < r_{\max} \\ \sum_{q=0}^{N} \pi_{l,i_q} & , i_q = (r_{\max}, q) \text{ for } l = r_{\max} \end{cases} \tag{4}$$

The probability of being in $(l,0)$ after l transition attempts is $\pi_{l,i}$ where $i=(l,0)$. If $l=r_{max}$ we sum up all probabilities for being in (r_{max},q), because for the time needed it is irrelevant, if this transmission attempt is successful or not.

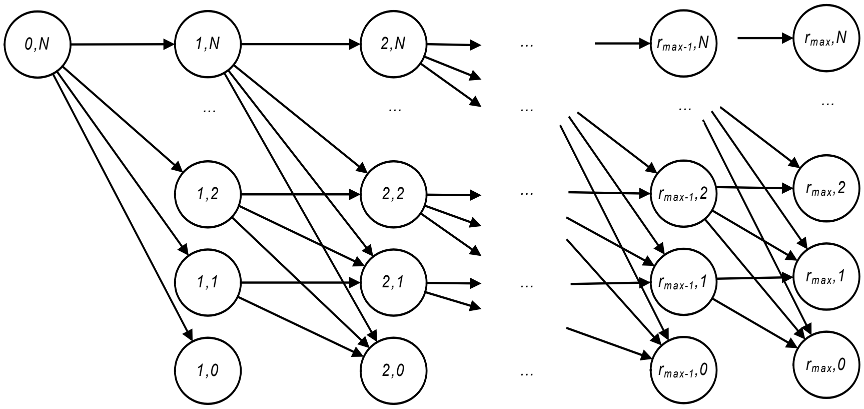

Figure 3. State transition diagram of the acyclic DTMC defining the pmf for $P_{att}(l)$.

C. Calculation of the transition probabilities for the binary symmetric channel model

To derive the remaining transition probabilities of the transition matrix $\boldsymbol{P}$ for the binary symmetric (BS) channel model, we assume independently and identically distributed bit errors with a bit error rate b_{err}. Given a subframe size of s bits the probability p_f that a subframe is lost is then given by

$$p_f = 1 - (1 - b_{err})^s \tag{5}$$

Assuming independent losses, the random variable S_N, denoting the lost subframes, follows a binomial distribution $b(N, p_f)$. Given the subframe loss probability p_f, the probability that out of N subframes are lost is given by

$$P_{BS}[S_N = k] = \binom{N}{k} p_f^{\,k} (1 - p_f)^{N-k} \tag{6}$$

Furthermore, the expected number of lost subframes in a transmission with N aggregated frames is

$$E_{BS}[S_N] = Np_f \tag{7}$$

D. Calculation of the transition probabilities for the Gilbert-Elliot channel error model

Next we derive the remaining transition probabilities of the transition matrix $\boldsymbol{P}$ for the Gilbert-Elliot channel (GE) model, which takes the bursty nature of the wireless channel into account. We need to derive the probability that k out of N subframes are lost under the Gilbert-Elliot channel model. We define the model to run on a "per-subframe" basis, meaning that it models the probability of a correct reception of a subframe and that state transitions of the Markov chain can occur after the transmission of a subframe. Note that this is also in conjunction with assumptions in previous work, e.g. [14]. The Gilbert-Elliot model consists of a state g ("good state") and a state b ("bad state"). When in the good state, subframe errors occur with a small error rate denoted as p_g, while when being in the bad state, subframe errors occur with a higher error rate of p_b. The probability of being in good or bad state is governed by the DTMC depicted in Figure 4.

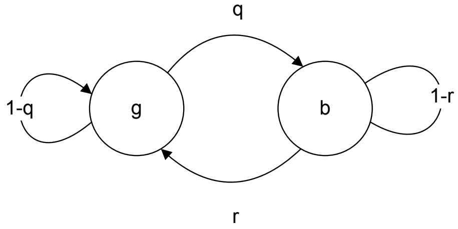

Figure 4. State transition diagram of the DTMC underlying the Gilbert-Elliot model.

This DTMC can be fully specified by the two parameters q and r, the state transition probabilities for going to the bad or the good state, respectively. These parameters and the related subframe error rates can be extracted out of real trace data for example. According to [15], we calculate the steady state probability $\tilde{\pi}_g$ for being in good state and the steady state probability for being in bad state $\tilde{\pi}_b$, by

$$\begin{aligned} \tilde{\pi}_g &= \frac{r}{r+q}, \\ \tilde{\pi}_b &= \frac{q}{r+q} \end{aligned} \tag{8}$$

To get the probability that k out of N subframes are correctly transmitted under this model, we formulate the two-dimensional DTMC depicted in Figure 5. This DTMC counts the correctly received frames by extending the Gilbert-Elliot model depicted in Figure 4.

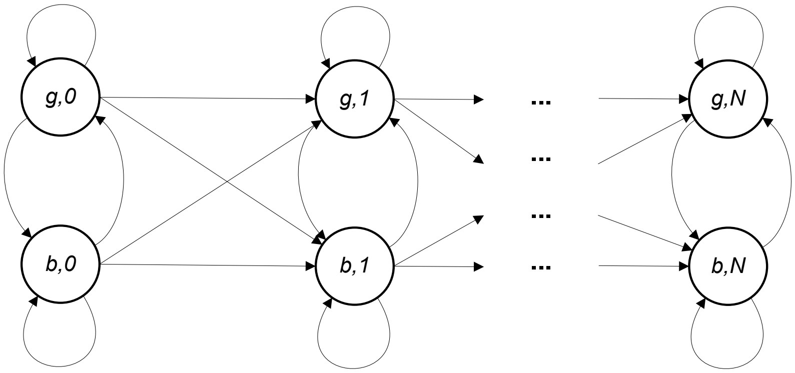

Figure 5. State transition diagram of the DTMC counting correctly received frames.

When in good state *(g,i),* $0 \le i < N$, four transitions can occur. First, with probability *(1-q)p$_g$* the DTMC resides in state *(g,i)*, because the transmitted frame was erroneous. Second, with probability *(1-q)(1-p$_g$)* the transmission was correct and there is a transition to state *(g,i+1)*, as one more subframe was correctly received. Then, with probability *qp$_g$* the subframe contains errors and the channel changes to bad state *(b,i)*. Finally there can be a successful transmission after whom the channel changes to bad state *(b,i+1)*. Therefore with probability *q(1-p$_g$)* the DTMC changes to *(b,i+1)*. Note, that for the last state *(g,N)* there is only the possibility, to stay in that state or to leave to the bad state, with probability *q-1* and *q*, respectively.

The transition probabilities for the bad states can be derived accordingly. Putting it all together, we get the probability matrix $\boldsymbol{P'}=[p'_{ij}]$, $i=(i_1,i_2)$ and $j=(j_1,j_2)$ for the DTMC of Figure 5 with

$$p'_{ij} = \begin{cases} q \cdot p_g & \text{for } i_1 = g, j_1 = b, j_2 = i_2 \text{ and } 0 \le i_2 < N \\ (1-q)(1-p_g) & \text{for } i_1 = g, j_1 = g, j_2 = i_2 + 1 \text{ and } 0 \le i_2 < N \\ (1-q)p_g & \text{for } i_1 = g, j_1 = g, j_2 = i_2 \text{ and } 0 \le i_2 < N \\ q(1-p_g) & \text{for } i_1 = g, j_1 = b, j_2 = i_2 + 1 \text{ and } 0 \le i_2 < N \\ 1-q & \text{for } i_1 = g, j_1 = g, j_2 = i_2 = \text{N} \\ q & \text{for } i_1 = g, j_1 = b, j_2 = i_2 = \text{N} \\ r \cdot p_b & \text{for } i_1 = b, j_1 = g, j_2 = i_2 \text{ and } 0 \le i_2 < N \\ (1-r)(1-p_b) & \text{for } i_1 = b, j_1 = b, j_2 = i_2 + 1 \text{ and } 0 \le i_2 < N \\ (1-r)p_b & \text{for } i_1 = b, j_1 = b, j_2 = i_2 \text{ and } 0 \le i_2 < N \\ r(1-p_b) & \text{for } i_1 = b, j_1 = g, j_2 = i_2 + 1 \text{ and } 0 \le i_2 < N \\ 1-r & \text{for } i_1 = b, j_1 = b, j_2 = i_2 = \text{N} \\ r & \text{for } i_1 = b, j_1 = g, j_2 = i_2 = \text{N} \\ 0 & \text{else} \end{cases} \tag{9}$$

We need this DTMC to calculate the probability that *k* out of *N* subframes are correctly received. We then use these probabilities to derive the opposite probability that *k* out of *N* subframes are lost, needed in (2). For our framework model, we assume that before each transmission attempt the Gilbert-Elliot model is in steady state, as the MAC carrier sensing function can not distinguish between good or bad channel state. Hence, using the steady state probabilities given by (8), we set the initial distribution row vector $\boldsymbol{\pi'_0}$ to

$$\pi'_{0,i} = \begin{cases} \tilde{\pi}_g & \text{for } i = (g,0) \\ \tilde{\pi}_b & \text{for } i = (b,0) \\ 0 & \text{else} \end{cases} \tag{10}$$

The desired probability $P_{GE}[S_N=k]$ that *k* out of *N* subframes are lost, can be derived by summing up the probabilities of being in *(g,N-k)* or *(b,N-k)* after *N* steps in the DTMC, that is

$$P_{GE}[S_N = k] = \boldsymbol{\pi'_0} \cdot \mathbf{P'}^N \cdot \mathbf{e}_{N-k} \tag{11}$$

with $\boldsymbol{\pi'_0}$ and $\boldsymbol{P'}$ given by (10) and (9), respectively, and $\boldsymbol{e}_i$ being a column vector of length *2(N+1)* with ones at *(g,i)* and *(b,i)* and zero else.

Furthermore, using the steady state probabilities of the model defined in (8), the expected number of lost subframes, when *N* aggregated subframes are transmitted, can be derived by

$$E_{GE}[S_N] = N(\tilde{\pi}_g \cdot p_g + \tilde{\pi}_b \cdot p_b) \tag{12}$$

E. Calculation of the transmission costs

After deriving the probabilities and the expected number of retransmissions, we now want to calculate the related costs for *l* transmission attempts. Let therefore *C(l)* denote the amount of time required to transmit one aggregated frame in exactly *l* rounds. *C(l)* splits into a term, needed in every transmission (T_{const}) accounting for the constant MAC overhead and a term, dependent on the actual retransmit attempt ($T_{ret}(l)$). Then *C(l)* is recursively defined by

$$C(l) = \begin{cases} 0 & , l = 0 \\ T_{ret}(l) + T_{const} + C(l-1) & , \text{for } 0 < l \le r_{max} \end{cases} \tag{13}$$

where T_{const} and T_{ret} are defined by

$$T_{const} = T_{DIFS} + T_{PHY} + T_{SIFS} + T_{ACK} \tag{14}$$

$$T_{ret}(l) = \frac{\min(2^{l-1} cw_{min}, cw_{max})}{2} T_{slot} + \frac{s \cdot S(l)}{B_{DATA}} \tag{15}$$

Note that T_{ret} takes the expected time needed due to the IEEE 802.11 backoff mechanism and the expected time for retransmitting the erroneous subframes into account. *S(l)* denotes the expected number of subframes that have to be retransmitted in the *l*-th round and depends on the used channel error model. In our two cases *S(l)* is defined using (7) and (12) as

$$S(l) = \begin{cases} N p_f^{\,l-1} & \text{for BS channel model} \\ N(\tilde{\pi}_g \cdot p_g + \tilde{\pi}_b \cdot p_b)^{l-1} & \text{for GE channel model} \end{cases} \tag{16}$$

We combine the probability for *l* needed transmissions $P_{att}(l)$ defined in (4) and the related costs *C(l)* defined in (13) for this event. Let T_{onehop} be the amount of time to transmit one aggregated frame (including time for retransmissions) over one hop. The expected value of T_{onehop} is given by

$$E[T_{onehop}] = \sum_{l=1}^{r_{max}} P_{att}(l) \cdot C(l) \tag{17}$$

We use the expected time for a complete transmission, to derive the maximum rate, at which the sender can transmit. For a multi-hop path, we assume that two nodes interfere with each other, when their distance is less than d_{coll} hops. Therefore, given a multi-hop path of length *h* hops, two nodes can transmit simultaneously if their distance is at least d_{coll} hops. Suppose the sender wants to transmit aggregated frames, with *N* subframes each of size *s* and let *size(N,s)* denote the size in bit of one aggregated frame. Then under these assumptions the sending rate w_{max} is given by

$$w_{\max} = \frac{size(N,s)}{\min(d_{coll}, h) \cdot E[T_{onehop}]} \tag{18}$$

V. MODEL VALIDATION BY SIMULATION

A. Simulation Setup

We implemented the IEEE 802.11n frame aggregation and block acknowledgement scheme as extension of the normal 802.11 MAC layer for the ns-2 [16] network simulator. We implemented the A-MPDU aggregation scheme and the compressed block acknowledgement scheme according to IEEE 802.11n specification. Issues left open by the specification, have been implemented according to the 802.11n functions of the Linux ATH9K kernel driver [17]. As routing protocol AODV is used. All simulation parameters are set according to Table III. In ns-2, all link-layer parameters of IEEE 802.11 are configured to provide a transmission range of 250m and a carrier sensing range as well as an interference range of 550m. The RTS/CTS handshake is disabled and we consider a channel bandwidth of 300 Mbit/s according to IEEE 802.11n while setting the size of transport data packets to 1,460 bytes. We further extended ns-2 to support both channel error models introduced in section IV. For the binary symmetric channel model this was done by randomly marking subframes as erroneous according to the fixed subframe error rate. For the Gilbert-Elliot channel model, consistent with our assumptions, we marked subframes according to the state related subframe error rate.

Consistent with the analytical model we consider an equally spaced multi-hop chain comprising $h+1$ nodes (h hops) with a single flow and a 200m inter-node distance. UDP packets traverse along the chain from the leftmost node (i.e., the source) to the rightmost node (i.e., the destination). Nodes in the chain are positioned such that only direct neighbors can communicate with each other over one hop.

We conduct steady-state simulations starting with an initially idle system. In each run, we utilize UDP traffic until 55,000 packets are successfully transmitted, and split the output of the experiment in 11 batches, each 5,000 packets in size. The first batch is discarded as initial transient. The considered performance measures are derived from the remaining 10 batches with 95% confidence intervals by the batch means method.

B. *Model Validation*

To validate the proposed analytical model we examined the mean number of transmissions needed to successfully transfer a frame. We compared the simulation results with those obtained from our Markov model. It can be seen in Figure 6 and Figure 7 that the results from our Markov model are indeed very close to simulation results. While for the BS channel model the bit error rate is the only parameter, for the GE channel model, there are four parameters, namely the two rates of leaving the good or the bad state, q and r, respectively, and the related subframe error rates p_g and p_b. We defined 4 different parameter sets listed in Table II, where the channel conditions are getting worse from set to set.

In a second experiment we compare the results from the model to the maximum throughput achievable by optimized paced UDP (meaning that the sender always transmits a fully aggregated frame). As we can observe in Figure 8, the analytical model is able to closely estimate the achievable throughput on a multi-hop path without as well as with bit errors. Note that with the existence of bit errors the maximum achievable goodput is slightly lower in ns-2 due to the lack of perfect synchronization as assumed by our model.

TABLE II. PARAMETER SETS FOR MODEL VALIDATION

	#1	*#2*	*#3*	*#4*
q	0.05	0.1	0.1	0.3
r	0.7	0.5	0.5	0.3
p_g	0	0	0.1	0.1
p_b	0.3	0.5	0.5	0.7

TABLE III. SIMULATION PARAMETERS

Symbol	***Value***
S	12272 bit (1534 Byte=1460 Byte payload + headers)
p_f	variable
q, r, p_g, p_b	variable (according to Table II)
N	42 (max. number of subframes of size 1534 Byte)
r_{max} *(ShortRetryLimit_)*	7
T_{slot} *(SlotTime_)*	9µs
cw_{min} *(CWMin_)*	16
cw_{max} *(CWMax_)*	1024
T_{SIFS} *(SIFS_)*	16µs
T_{DIFS}	34µs
T_{ACK}	20.75µs
T_{PHY}	20µs
B_{DATA} *(bandwidth_)*	300 Mbit/s
*PreambleLength_*	72 bit
*PLCPDataRate_*	6 Mbit/s

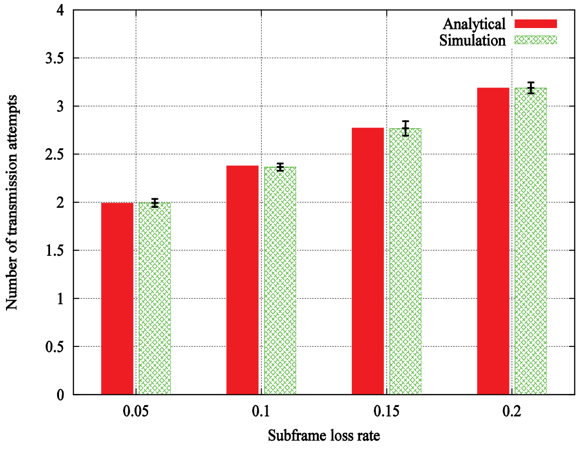

Figure 6. Validation of the analytical model for the binary symmetric channel model with respect to number of transmissions.

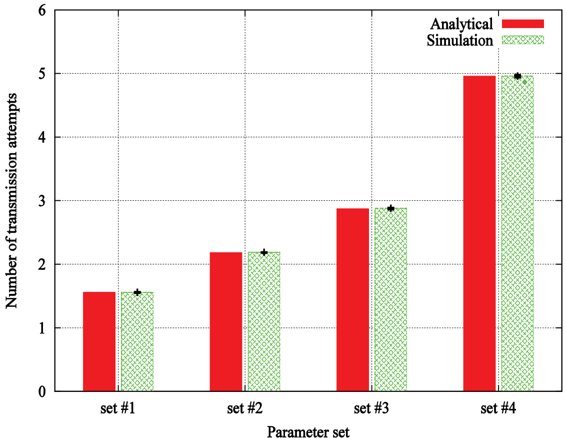

Figure 7. Validation of the analytical model for the Gilbert-Elliot channel model with respect to number of transmissions with parameter sets according to Table II.

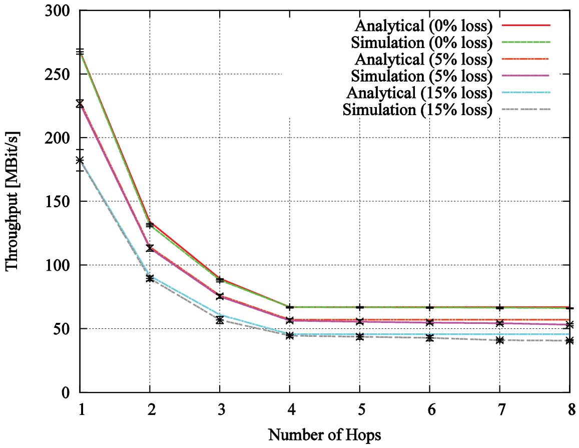

Figure 8. Validation of the analytical model for different subframe error rates with respect to throughput.

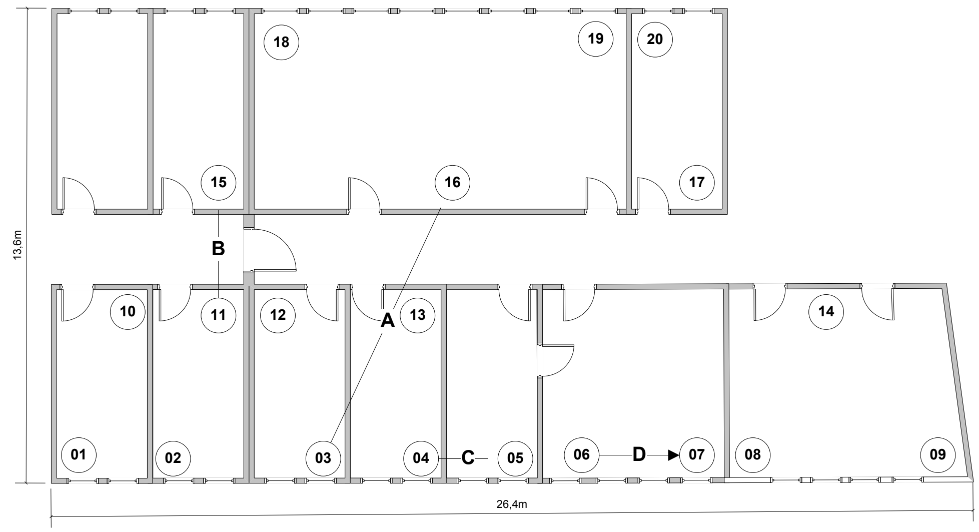

Figure 9. Indoor MIMO Mesh Testbed with indicated links of Table V

VI. MODEL EVALUATION IN AN INDOOR TESTBED

A. Testbed Setup

Our Indoor MIMO Mesh Testbed comprises 20 wireless mesh nodes located in 10 rooms in the department building covering roughly 250 m². An overview of the testbed with the node locations is depicted in Figure 9. Each node consists of a Siemens ESPRIMO P2510 PC with an Intel Celeron 3.2 GHz processor, 512 MB RAM, 80 GB HDD and a D-Link DWA-547 wireless PCI network interface card (NIC). This NIC is equipped with three 5dBi omnidirectional antennas and an AR 9223 Atheros chipset, able to support 802.11n-based MIMO communication in the 2.4 GHz band. Each node runs openSUSE 11.2 as operating system with a modified kernel based on version 2.6.34.

As device driver for the wireless NIC, we employ the *ath9k* driver for Atheros chipsets. To allow remote management of the nodes, each node possesses a Gigabit Ethernet NIC, connected to the subnet of the University of Leipzig through a Gigabit switch. Hence, wireless experiments can be managed from a remote computer and traces can be copied and evaluated through the wired network. Table IV shows a detailed description of hardware and software components of the testbed.

We needed to set up our cards both as normal interface and as a special monitoring interface that allows capturing management and erroneous frames. Furthermore, we implemented a tracing module that logs the MAC sequence numbers of each subframe per aggregate and which ones were erroneous and had to be retransmitted. This data log was later used to map frames on the receiver side with the appropriate frames on the transmitter. We assured that the CPU and IO overhead arising by the tracing do not effect IEEE 802.11n operation by conducting various validation experiments.

TABLE IV. TESTBED OVERVIEW

Component	***Description***
PC	Siemens ESPRIMO P2510 Celeron 3.2 GHz, 512 MB RAM, 80 GB HDD
Wireless Card	D-Link DWA-547 PCI NIC equipped with 3 antennas
Chipset	Atheros AR 9223, operating at 2.4 GHz
Operating System	openSUSE 11.2 with kernel version 2.6.34

TABLE V. LINK PROPERTIES

Link label	***Physical data rate***	***Model parameter***			
		q	r	p_g	p_b
A	120 Mbit/s	0.0005	0.0704	0.0000	0.8805
B	150 Mbit/s	0.0054	0.0839	0.0014	0.9400
C	180 Mbit/s	0.0024	0.0832	0.0011	0.7734
D	300 Mbit/s	0.0039	0.1508	0.0179	0.8679

B. Validation Metholodgy

For our experimental measurement study, we used the links A to D of our Indoor MIMO Mesh Testbed depicted in Figure 9. We chose the links to take different link qualities into account being link D the link with the best link quality and link A the one with the worst. We configured nodes 03, 04, 06 and 11 to run in client mode and nodes 05, 07, 15 and 16 to run in access point mode, respectively. Note that due to the increased complexity of IEEE 802.11n, multi-hop ad-hoc mode isn't realized in the Linux *ath9k* kernel yet. Hence, we conducted all our experiments in 1-hop infrastructure mode. To take the different link qualities into account, IEEE 802.11n offers different Modulation and Coding Schemes (MCS) that result in different available data rates on the physical layer. We fixed the MCS classes to 5, 7, 12, and 15 for link A, B, C, and D, respectively, resulting in the physical data rates reported in Table V. We chose these MCS classes as they offer the best goodput for the given link. Note that the reported subframe error rates depend on the chosen MCS class, as different forward error correction rates and modulation schemes are employed.

We used the bandwidth measurement tool iperf for Linux [18] to create saturated UDP traffic at the sender with a payload size of 1460 bytes. We chose UDP traffic to limit the influence of the TCP exponential backoff mechanism that may degrade the throughput. Because our devices run in the 2.4 GHz band we estimated the impact of interference. Therefore, we ran a one-week long-term experiment measuring the goodput on a sensitive link to identify time slots with the least external interference. We noticed that during the working hours between 8am and 8pm, the measured goodput was strongly influenced by external interference, especially due to students who access the web wirelessly through their IEEE 802.11 equipped laptops. To our regret, also apart of these times we registered little interference due to 802.11b/g background traffic because of a wireless transmitting video surveillance system installed in a nearby computer pool. However, we conduct our experiments during these times with fewer external influences.

We conducted fixed length measurement experiments starting from an initially idle system. Each experiment lasted 60 seconds. We halve the measurement data and used the first half for the training of the Gilbert-Elliot model and the second one to derive the considered performance measure. We employed the well-known Baum-Welch algorithm [19] for the parameter fitting of the underlying Gilbert-Elliot channel model. From the training data we derived a binary sequence characterizing the status of the received frame, 0 for correctly received and 1 for an erroneous reception. Then, we used this sequence as input for the Baum-Welch algorithm.

C. Measurement Results

We show the applicability of the Gilbert-Elliot model for characterizing the channel state in IEEE 802.11n in two steps. First, we show that the reception of correctly and erroneous subframes is nearly uncorrelated in the observed trace data. This is necessary as the used Gilbert-Elliot model is a Markov model and state changes only depend on the current state and not on any history. As an example, one may argue that longer runs of correctly received subframes may lead to a shorter length of the consecutive erroneous reception run. However, this behavior could not be modeled with the Gilbert-Elliot channel model. Therefore, we extracted the burst lengths of correctly respectively erroneous received subframes. We define a burst to be a run of consecutive correctly respectively erroneous receptions of subframes. Now we form pairs of directly consecutive bursts. For example, the binary sequence "00010011" would lead to the pairs (3,1) (2,2) saying that after 3 correctly received subframes one erroneous subframe was received and afterwards after 2 correctly received subframes 2 erroneous received subframes followed. To evaluate whether a hidden correlation exist between the burst lengths we plot these pairs in Figure 10. We see that no obvious relation exists for the burst lengths. Note, that the higher density of pairs near the point of origin is a result of the increased probability of shorter runs compared to longer runs. To further examine the dependence between the burst lengths we derive the Pearson correlation coefficient *r* [20], defined by

$$r = \frac{\sum_{i=1}^{n}(X_i^C - E(X^C)) \cdot (X_i^E - E(X^E))}{\sqrt{\sum_{i=1}^{n}(X_i^C - E(X^C))^2} \cdot \sqrt{\sum_{i=1}^{n}(X_i^E - E(X^E))^2}} \tag{19}$$

where X^C and X^E are the pairwise burst lengths of correctly respectively erroneous received subframes, with E(·) being their mean value and *n* the number of sample pairs.

The Pearson correlation coefficient is a normalized metric detecting a (positive or negative) linear correlation between data pairs. While for perfectly linear correlation this coefficient is 1, it is 0 for completely uncorrelated data pairs. The calculated correlation coefficients depicted in Table VI are quite small for all links, thus indicating nearly no correlation.

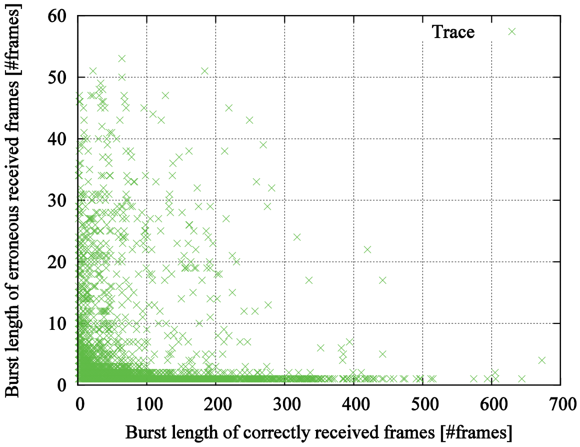

Figure 10. Scatter plot of the lengths of consecutive bursts for link D

As our second step, we now compare different measurements derived from trace data of the testbed with those derived with the model. Hence, we compare in Table VI the mean subframe error rate, the mean burst length of correctly received subframes and the mean burst length of erroneous received subframes, respectively. Especially the burst lengths of erroneous received subframes are important for transport and application layer protocols, as long bursts may lead to performance degradations. As an example the throughput of a TCP connection severely degrades if many subsequent packet losses occur because of the exponential backoff mechanism.

We observe that the mean subframe error rates of the trace data and the Gilbert-Elliot model are quite similar for all links. Only for link D a greater derivation can be observed. Furthermore, we notice that also the mean burst lengths are similar for all links, although the model sometimes underestimates these lengths. We think the deviations are mainly due to the different data sets used for calculation. For training the Gilbert-Elliot model, we use the first 30 seconds of our experiment, while for calculating the measured mean values we use the second 30 seconds. Because of the time varying channel conditions differences between these values are understandable.

Now we take a closer look at the exact distribution of the lengths of error bursts. While we can directly extract this data out of the trace, we have to gather this information by simulating the Gilbert-Elliot model first. We plot in Figure 11 the complementary cumulative distribution function of the burst length of erroneous received subframes. We observe that the probability for bursts larger than 30 subframes is small, e.g. only one percent.

TABLE VI. LINK STATISTICS

Link label	*A*	*B*	*C*	*D*
Correlation coefficient r according to (19)	0.166	0.328	0.021	0.044
Mean subframe error rate	0.0059	0.0487	0.0203	0.0516
Predicted subframe error rate	0.0055	0.0583	0.0224	0.0392
Mean burst length of correct subframes	1112.3	120.3	159.1	33.1
Predicted burst length of correct subframes	717.3	103.6	122.5	41.5
Mean burst length of erroneous subframes	6.63	6.17	3.30	1.80
Predicted burst length of erroneous subframes	5.75	6.24	2.89	1.77

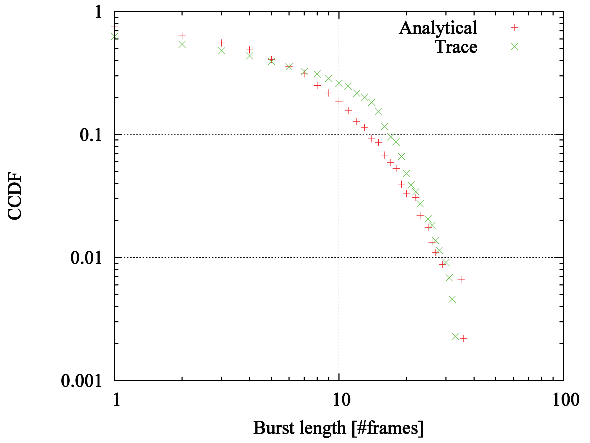

Figure 11. Complementary cumulative distribution function of the burst length of erroneous received frames for link B

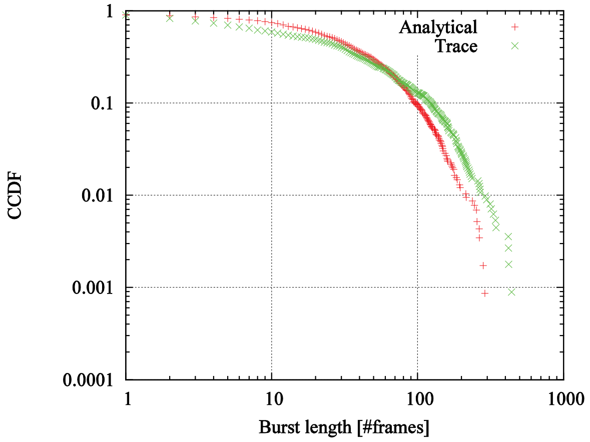

Figure 12. Complementary cumulative distribution function of the burst length of correctly received frames for link D

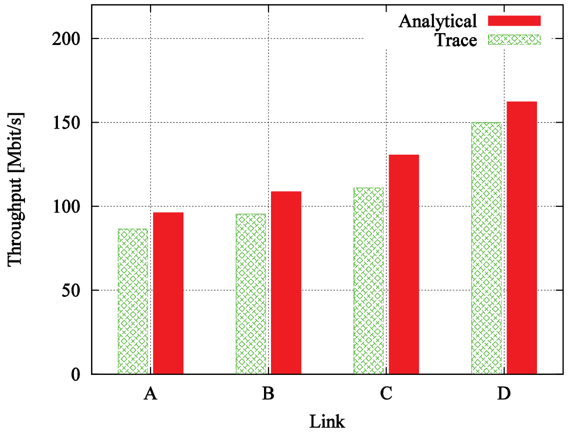

Figure 13. Comparison of the analytical derived and the actual achieved throughput for different links according to Table V

In Figure 12, we take a closer look at the distribution of the burst lengths of the correctly received subframes. We plot the complementary cumulative distribution function of the burst length of correctly received subframes for link D. We notice that although the shape of the curve is similar, the burst lengths are way larger compared to the ones of Figure 11. This is due to the small subframe error probability of only 5% on that link. We also observe that in both figures the Gilbert-Elliot model matches the trace data quite well. We conclude that the Gilbert-Elliot model is a good choice to model channel error probabilities with IEEE 802.11n, not only because of the good matches we could achieve, but also because of its simplicity and analytical tractability.

Finally, in Figure 13 we compare the real measured and the analytically derived throughput. We observe that the actual achieved throughputs are much smaller compared to our simulation results. This is due to several reasons. First, after analyzing the aggregation logs and referring to the Atheros specification we realized that our used chipset is only able to aggregate 32 subframes per frame opposed to 64 reported in the standard [1]. Secondly, as our devices run in the 2.4 GHz band they run in a compatibility mode with legacy IEEE 802.11b/g devices. Therefore, some parameters differ to those reported in Table III. According to the standard, the slot time T_{slot} and the transmit duration of the physical header T_{PHY} are increased to 20µs and 40µs, respectively. We updated these values in our model, but still our analytical results are larger than the actual achieved throughputs. We believe this is mainly due to the explained interference of the wireless video surveillance system. Though direct collisions may be unlikely the increased channel utilization leads to increased channel access times not captured by our model. We think that our model still can be employed as a good indicator for the achievable throughput as the observed derivations lie between 5% and 20%.

VII. Conclusion

In this paper we characterized the effective throughput for multi-hop paths in IEEE 802.11n based wireless mesh networks. We derived an analytical model based on a Markov chain capturing the effects of frame aggregation and block acknowledgements. Our model calculates the expected number of retransmissions by estimating the amount of subframes to be retransmitted under a given channel model. We showed how to integrate the well-known Gilbert-Elliot channel model into our model to take complex error characteristics into account. We validated our model through simulations and quantitatively evaluate it in an indoor wireless testbed. Furthermore, we showed that the Gilbert-Elliot channel model is able to characterize error behavior in IEEE 802.11n communication.

Currently we are implementing Linux kernel extensions to enable multi-hop communication to further evaluate our model on multi-hop paths.

References

[1] IEEE 802.11n: Standard for Wireless LAN Medium Access Control (MAC) and Physical Layer (PHY) Specifications Amendment 5: Enhancements for Higher Throughput, 2009.

[2] A. Banchs and L. Vollero, Throughput Analysis and Optimal Configuration of 802.11e EDCA, *Computer Networks*, **50**, 2006.

[3] G. Bianchi, Performance Analysis of the IEEE 802.11 Distributed Coordinated Function, *IEEE JSAC*, **18**, 2000.

[4] E. Engelstad and O. Østerbø, Non-Saturation and Saturation Analysis of IEEE 802.11e EDCA with Starvation Prediction, *Proc. ACM MSWiM*, 2005.

[5] F. Daneshgaran, M. Laddomada, F. Mesiti, and M. Mondin, Unsaturated throughput analysis of IEEE 802.11 in presence of non ideal transmission channel and capture effects, *IEEE Transactions on Wireless Communications*, **7**, 2008.

[6] T. Li, Q. Ni, D. Malone, D. Leith, Y. Xiao, and R. Turletti, Aggregation with Fragment Retransmission for Very High-Speed WLANs, *IEEE/ACM Transactions on Networking*, **17**, 2009.

[7] K. Chen, Y. Xue, S. Shah, and K. Nahrstedt, Understanding Bandwidth-Delay Product in Mobile Ad Hoc Networks, *Computer Communications*, **27**, 2004.

[8] Z. Fu, H. Luo, P. Zerfos, S. Lu, L. Zhang, and M. Gerla, The Impact of Multihop Wireless Channel on TCP Performance. *IEEE Transactions on Mobile Computing*, **4**, 2005.

[9] V. Shrivastava, S. Rayanchu, J. Yoonj, and S. Banerjee, 802.11n Under the Microscope, *Proc. ACM IMC*, 2008.

[10] J. Karlsson and A. Kassler, A. Brunstrom, Impact of Packet Aggregation on TCP Performance in Wireless Mesh Networks, *Proc. IEEE HotMESH*, 2009.

[11] S. ElRakabawy, S. Frohn, and C. Lindemann, A Scalable Dual-Radio Wireless Testbed for Emulating Mesh Networks, *Springer Wireless Networks*, **16**, 2010.

[12] E. O. Elliott, Estimates of error rates for codes on burst-noise channels, *Bell Syst. Tech. J.*, **42**, 1963.

[13] S. Frohn, S. Gübner, and C. Lindemann, Analyzing the Effective Throughput in Multi-Hop IEEE 802.11n Networks*, Proc. IEEE HotMESH*, 2010.

[14] P. Bhagwat, P. Bhattacharya, A. Krishna, and S. K. Tripathi, Using channel state dependent packet scheduling to improve TCPthroughput over wireless LANs, *Springer Wireless Networks*, **3**, 1997.

[15] M. Zorzi and R. R. Rao, On the Statistics of Block Errors in Bursty Channels, *IEEE Transactions on Communications*, **45**, 1997.

[16] K. Fall and K. Varadhan (Ed.), The ns-2 Manual, Technical Report, The VINT Project, UC Berkeley, LBL, and Xerox PARC, 2007.

[17] Linux Wireless ATH9K Kernel Driver, http://linuxwireless.org/en/users/Drivers/ath9k, 2010.

[18] Iperf, the TCP/UDP Bandwidth Measurement Tool, http://dast.nlanr.net/projects/iperf/.

[19] L. E. Baum, T. Petrie, G. Soules, and N. Weiss, A Maximization Technique Occurring in the Statistical Analysis of Probabilistic Functions of Markov Chains, *The Annals of Mathematical Statistics*, **41**, 1970.

[20] R. M. Mickey, O. J. Dunn, and V. A. Clark, Applied Statistics: Analysis of Variance and Regression, New York, Wiley, 2004.